© 2015. Published by The Company of Biologists Ltd | The Journal of Experimental Biology (2015) 218, 915-922 doi:10.1242/jeb.116780

RESEARCH ARTICLE

Spectral sensitivity in Onychophora (velvet worms) revealed by electroretinograms, phototactic behaviour and opsin gene expression

Holger Beckmann[1,2,*], Lars Hering[1], Miriam J. Henze[3], Almut Kelber[3], Paul A. Stevenson[4] and Georg Mayer[1,5]

ABSTRACT

Onychophorans typically possess a pair of simple eyes, inherited from the last common ancestor of Panarthropoda (Onychophora+Tardigrada+Arthropoda). These visual organs are thought to be homologous to the arthropod median ocelli, whereas the compound eyes probably evolved in the arthropod lineage. To gain insights into the ancestral function and evolution of the visual system in panarthropods, we investigated phototactic behaviour, opsin gene expression and the spectral sensitivity of the eyes in two representative species of Onychophora: *Euperipatoides rowelli* (Peripatopsidae) and *Principapillatus hitoyensis* (Peripatidae). Our behavioural analyses, in conjunction with previous data, demonstrate that both species exhibit photonegative responses to wavelengths ranging from ultraviolet to green light (370–530 nm), and electroretinograms reveal that the onychophoran eye is maximally sensitive to blue light (peak sensitivity ~480 nm). Template fits to these sensitivities suggest that the onychophoran eye is monochromatic. To clarify which type of opsin the single visual pigment is based on, we localised the corresponding mRNA in the onychophoran eye and brain using *in situ* hybridization. Our data show that the *r-opsin* gene (*onychopsin*) is expressed exclusively in the photoreceptor cells of the eye, whereas *c-opsin* mRNA is confined to the optic ganglion cells and the brain. Together, our findings suggest that the onychopsin is involved in vision, whereas c-opsin might have a photoreceptive, non-visual function in onychophorans.

KEY WORDS: Arthropod, Eye, Light response, Vision, Opsins, Phototaxis, Evolution

INTRODUCTION

Onychophorans (velvet worms) typically bear a pair of simple, ocellus-like eyes (Fig. 1A,B), which are thought to be homologous with the median ocelli of arthropods (Mayer, 2006), one of their closest relatives (Giribet and Edgecombe, 2012). Accordingly, the last common ancestor of Panarthropoda (Onychophora+Tardigrada+Arthropoda) most likely possessed a pair of ocellus-like visual organs, whereas the compound eyes evolved within the arthropod lineage (Mayer, 2006; Hering et al., 2012; Hering and Mayer, 2014). Although arthropods typically have multiple rhabdomeric opsins (r-opsins) as components of visual pigments, their presence being a prerequisite for colour vision (reviewed by Briscoe and Chittka, 2001), transcriptomic analyses of the opsin repertoire revealed only one r-opsin gene (*onychopsin*) in five distantly related onychophoran species (Hering et al., 2012). In phylogenetic analyses, *onychopsin* forms the sister group to the visual r-opsins of arthropods, suggesting that the product of this gene functions in onychophoran vision. However, a ciliary-type opsin (c-opsin, to which type the visual opsins of vertebrates also belong; reviewed by Porter et al., 2012), has also been reported to occur in the onychophoran eye (Eriksson et al., 2013). Hence, a detailed expression study at the cellular level seems necessary to clarify whether r- or c-type opsins, or both, are involved in onychophoran vision.

Behavioural studies revealed negative phototactic behaviour in two species of Peripatidae: *Epiperipatus biolleyi* (see Monge-Nájera et al., 1993) and *Principapillatus hitoyensis* (referred to as *Epiperipatus* cf. *isthmicola* in Hering et al., 2012). Specimens of *P. hitoyensis* showed a photonegative reaction to wavelengths ranging from 363 nm (ultraviolet, UV) to 586 nm (yellow). The sensitivity maximum (α-peak) of the visual pigment in this species was therefore estimated to be in the blue-green range of the spectrum (Hering et al., 2012). However, neither the specific wavelength of the α-peak nor the actual spectral sensitivity curve of the onychophoran photoreceptors is known. Moreover, it is unclear whether a photonegative reaction to the same wavelengths occurs in representatives of the second major onychophoran subgroup, the Peripatopsidae, for which quantitative data are still missing.

We therefore analysed the behavioural response to light and localised the expression of the r- and c-type opsins in the peripatopsid *Euperipatoides rowelli*. To identify the sensitivity maximum (α-peak) of the visual pigment and to complement previous data from *P. hitoyensis*, we additionally performed electrophysiological recordings from the eye in both *E. rowelli* and *P. hitoyensis*. The data allow conclusions regarding the physiological properties and function of the visual system in the last common ancestor of Onychophora and Panarthropoda, respectively.

RESULTS

Spectral sensitivity of the onychophoran eye

We recorded electroretinograms (ERGs), extracellular, light-induced potential changes in the retina, from the eyes of six specimens of *E. rowelli* of both sexes and one male of *P. hitoyensis* (Fig. 2A,B). Responses to light flashes of 40 or 100 ms duration consisted of an initial hyperpolarisation truncated by a depolarisation (Fig. 3A,C). The half width of the response (width at half maximal hyperpolarisation) exceeded 140 ms and the time to peak (time interval from stimulus onset to maximal hyperpolarisation) exceeded 95 ms for all tested intensities. Both values increased considerably with decreasing

[1]Department of Animal Evolution and Development, Institute of Biology, University of Leipzig, Talstrasse 33, Leipzig D-04103, Germany. [2]Rudolf-Boehm-Institute of Pharmacology and Toxicology, University of Leipzig, Haertelstrasse 16–18, Leipzig D-04107, Germany. [3]Department of Biology, Lund University, Sölvegatan 35, Lund 22362, Sweden. [4]Department of Animal Physiology, Institute of Biology, University of Leipzig, Talstrasse 33, Leipzig D-04103, Germany. [5]Department of Zoology, Institute of Biology, University of Kassel, Heinrich-Plett-Str. 40, D-34132 Kassel, Germany.

*Author for correspondence (holger.beckmann@medizin.uni-leipzig.de)

Received 14 November 2014; Accepted 16 January 2015

The Journal of Experimental Biology (2015) 218, 915-922 doi:10.1242/jeb.116780

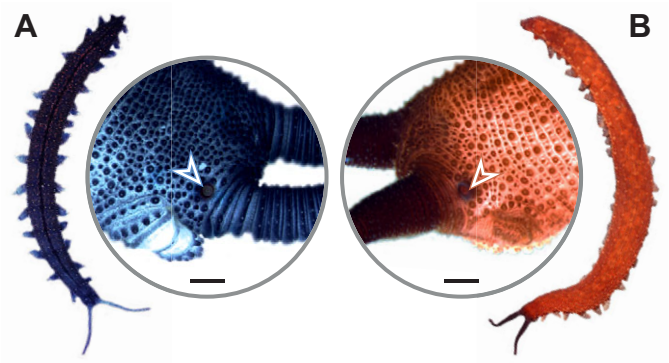

Fig. 1. Position of eyes in the onychophoran species *Euperipatoides rowelli* and *Principapillatus hitoyensis*. Both species possess a pair of simple lateral eyes, one at the base of each antenna (arrowheads). Scale bars: 500 µm. (A) The peripatopsid *E. rowelli*. (B) The peripatid *P. hitoyensis*. Details in A and B are from specimens preserved in 70% ethanol.

stimulus intensity (Fig. 3A,C). Spectral flashes with equal photon flux revealed that the dark-adapted retina was most sensitive to wavelengths around 480 nm, i.e. to the region of the spectrum perceived as blue by humans. We fitted template formulae (Govardovskii et al., 2000), which approximate the absorbance spectra of opsin-based visual pigments in invertebrates (Stavenga, 2010), to the data from each individual (Fig. 3B,D) and averaged the results for different individuals of the same species. Optimal fits were obtained assuming a visual pigment with an absorbance peak at 474±6.5 nm (wavelength λ_{max}, mean ± s.d.; coefficient of determination: R^2=0.88±0.03) for the six specimens of *E. rowelli* and at 484 nm (R^2=0.93) for one specimen of *P. hitoyensis*. When the eye was adapted to green light, responses were indistinguishable from background noise levels, and no other sensitivity peaks were apparent at shorter wavelengths. During recovery from green adaptation, the shape of the spectral curve was similar to the curve of the dark-adapted retina (supplementary material Fig. S1).

Localisation of r-opsin and c-opsin in the onychophoran eye and brain

To determine whether the signal obtained from the electrophysiological recordings is related to the onychophoran r- or c-type opsin, we performed fluorescence *in situ* hybridization experiments on cryosections of the *E. rowelli* heads (Fig. 4A–F). Our data show that *Er-onychopsin* is expressed in the photoreceptor layer of each eye, and lacking in other tissues, including the brain (*N*=6; Fig. 4B–D; supplementary material Fig. S2). In contrast, *Er-c-opsin* mRNA is localised both in optic ganglion cells within the eye and in numerous neuronal somata within the brain, in particular in the ventral perikaryal layer of the protocerebrum (Fig. 4E,F; supplementary material Fig. S2). A few additional cells expressing *Er-c-opsin* are seen in the deutocerebrum and in the medullary cords (=connecting cords) linking the brain to the ventral nerve cords (Fig. 4E,F). Most importantly, and in contrast to optic ganglion cells, *Er-c-opsin* mRNA is not expressed in the photoreceptor layer of the eye (Fig. 4E).

Our control experiments using the sense probe for *Er-onychopsin* revealed no signal within the eye, indicating that the labelling obtained using the antisense probe for *Er-onychopsin* is specific (supplementary material Fig. S2). The nonspecific labelling in the cuticle lining the epidermis and pharyngeal lumen, which occurs in

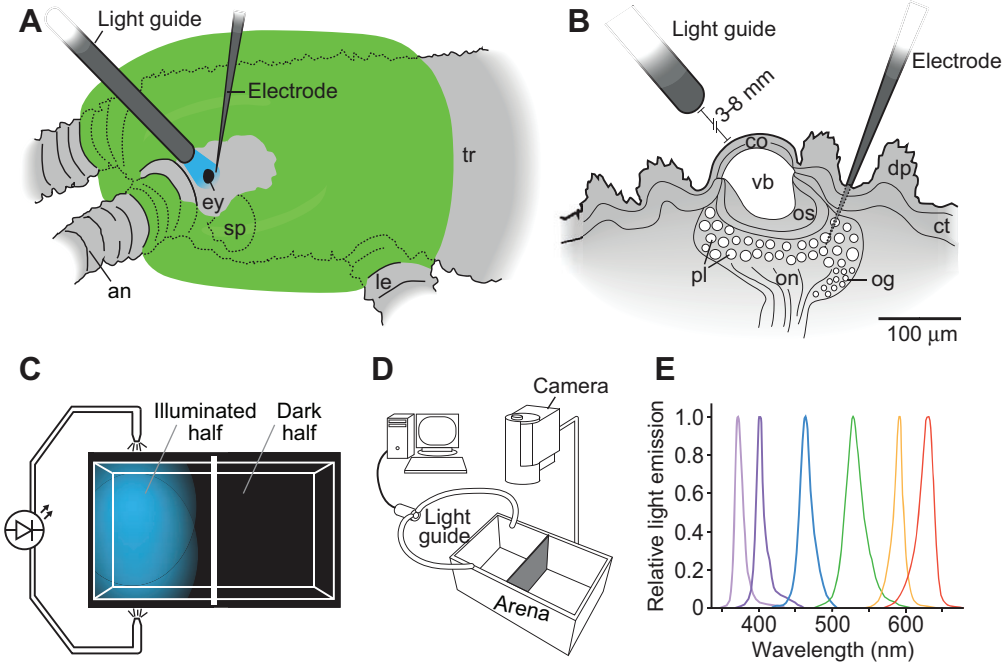

Fig. 2. Experimental design of the electrophysiological and behavioural experiments. (A) Diagram of an electrophysiological preparation. The head of a specimen is embedded in dental cement (green), so that only the area surrounding the eye is accessible for the electrode and the light guide (light cone indicated in blue). (B) Diagram of a sagittal section of the eye (based on a histological section from Mayer, 2006) illustrating the desired position of the electrode. Anterior is left. The electrode does not penetrate the cornea of the eye but is inserted through the adjacent cuticle and tissue. (C) Top view of the arena used for behavioural experiments. Only one half was illuminated (indicated in light blue). (D) Overview of the entire behavioural setup. (E) Normalised emission spectra of the narrow-banded light-emitting diodes used in the behavioural setup. Abbreviations: an, antenna; co, cornea; ct, connective tissue; dp, dermal papilla; ey, eye; le, leg; og, optic ganglion cells; on, optic neuropil; os, outer segments of photoreceptors; pl, perikaryal layer of photoreceptors; sp, slime papilla; tr, trunk; vb, vitreous body (=lens-like structure).

The Journal of Experimental Biology

The Journal of Experimental Biology (2015) 218, 915-922 doi:10.1242/jeb.116780

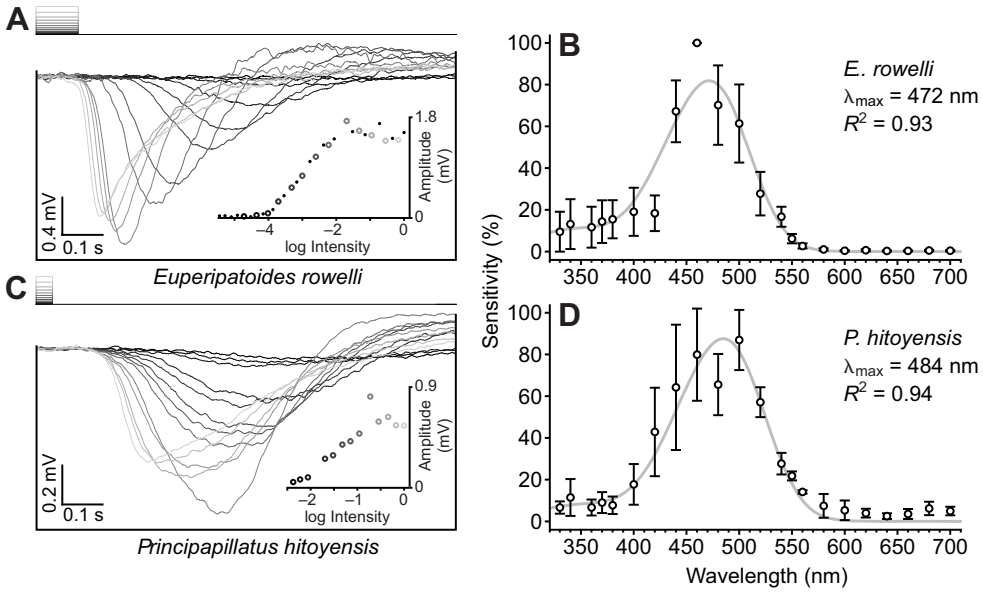

Fig. 3. Spectral sensitivity of the eye in the peripatopsid *E. rowelli* and the peripatid *P. hitoyensis* determined by electroretinograms (ERGs). (A,C) ERGs recorded for flashes of white light with increasing intensity (top trace) consisted of an initial hyperpolarisation truncated by a depolarisation (bottom trace). Response amplitudes (insets) were calculated as potential changes from the baseline at stimulus onset to maximal hyperpolarisation. Small dots in A represent measurements, for which no ERG is shown. (B,D) Averaged spectral sensitivity of the eye in two individuals (mean±s.d., six measurements per data point) based on response amplitudes to light stimuli of different wavelengths and equal photon flux. Fitting a template (grey line) for the absorbance of an opsin-based visual pigment to the measurements yielded a wavelength of peak absorbance (λ_{max}) of about 480 nm with a coefficient of determination (R^2) over 0.9 for both species.

all our preparations, is due to autofluorescence. In contrast, the *Er-c-opsin* sense probe revealed a similar pattern to the *Er-c-opsin* antisense probe (supplementary material Fig. S2). The same result was obtained repeatedly in all experiments using different sense probes on cryosections of different individuals (N=4), whereas an increase of the hybridization temperature to 58°C completely abolished the labelling in all reactions, irrespective of whether the sense or antisense probes were used.

Behavioural response of onychophorans to light of different wavelengths

To clarify whether *E. rowelli* shows negative phototaxis, single animals were released in a dark arena and left free to move in any direction. After directing a bright white light at their heads, the animals immediately changed walking direction away from the light source (Fig. 5A; Wilcoxon-signed-rank test: P<0.001), but did not veer from course in control experiments without the light stimulus (Fig. 5B).

To determine the sensitivity threshold of *E. rowelli*'s negative phototaxis, we used a blue-light-emitting diode (λ_{max}=465 nm, i.e. close to the sensitivity maximum obtained from the electroretinograms, cf. Fig. 3B). Up to 6 animals were grouped (N=7 groups) and released simultaneously in one half of a dark arena, after which this half was illuminated with blue light of four different intensities (3×10^{11}, 6×10^{11}, 9×10^{11}, 12×10^{11} photons cm^{-2} s^{-1}, measured at the bottom of the arena) and the behaviour of the animals was then recorded for 5 min. In our setup, no significant reaction to blue light was evident after an illumination with 3×10^{11} photons cm^{-2} s^{-1} and avoidance behaviour first occurred at 6×10^{11} photons cm^{-2} s^{-1} (Fig. 5C). Hence, to evaluate reactions to wavelengths outside the sensitivity maximum, the stimulus was delivered at twice the intensity of this value (i.e. 12×10^{11} photons cm^{-2} s^{-1}) in subsequent experiments.

To determine whether or not a shorter exposure to light would affect the significance of our results, we compared the animal's reaction to illumination for 5, 3, 2 and 1 min, respectively (supplementary material Fig. S3). The data show that illumination for 1 min is sufficient to elicit a highly significant avoidance reaction. However, since about one third of our animals did not respond to the 1 min stimulus, we selected an illumination duration of 2 min for the remaining experiments (Fig. 5C).

For our major experiments, we again released groups of up to six animals (N=15 groups) in one half of the dark arena, which was then illuminated with quasi-monochromatic light of six different wavelengths of the same intensity (12×10^{11} photons cm^{-2} s^{-1}). In these experiments, *E. rowelli* specimens significantly evaded wavelengths ranging from UV to green light (P<0.001; Friedman-test with Dunn's post-test) but showed no evasive reaction to light of longer wavelengths (P_{591}=0.343, P_{631}=0.650; Friedman test with Dunn's post-test) (Fig. 6A). In a final set of experiments, we tested our specimens for potentially positive phototaxis, because it is unknown whether or not they show preference for a particular wavelength. For these experiments, we used the same setting and released the animals in one half of the dark arena, but illuminated the other half with light of each of the six wavelengths, respectively. The obtained data gave no indication that the animals exhibit positive phototactic behaviour (Fig 6B; Friedman test with Dunn's post-test: P_{465} and P_{591}=0.769, P_{other}>0.999).

DISCUSSION

Onychophorans avoid wavelengths ranging from UV to green light

Our behavioural data provide evidence for negative phototaxis in the peripatopsid *E. rowelli*, corresponding to previous results from the peripatid *P. hitoyensis* (see Hering et al., 2012). In our tests, specimens of *E. rowelli* were not attracted by light but instead significantly avoided illumination with wavelengths ranging from UV to green light. The animals are unlikely to have reacted to heat

The Journal of Experimental Biology (2015) 218, 915-922 doi:10.1242/jeb.116780

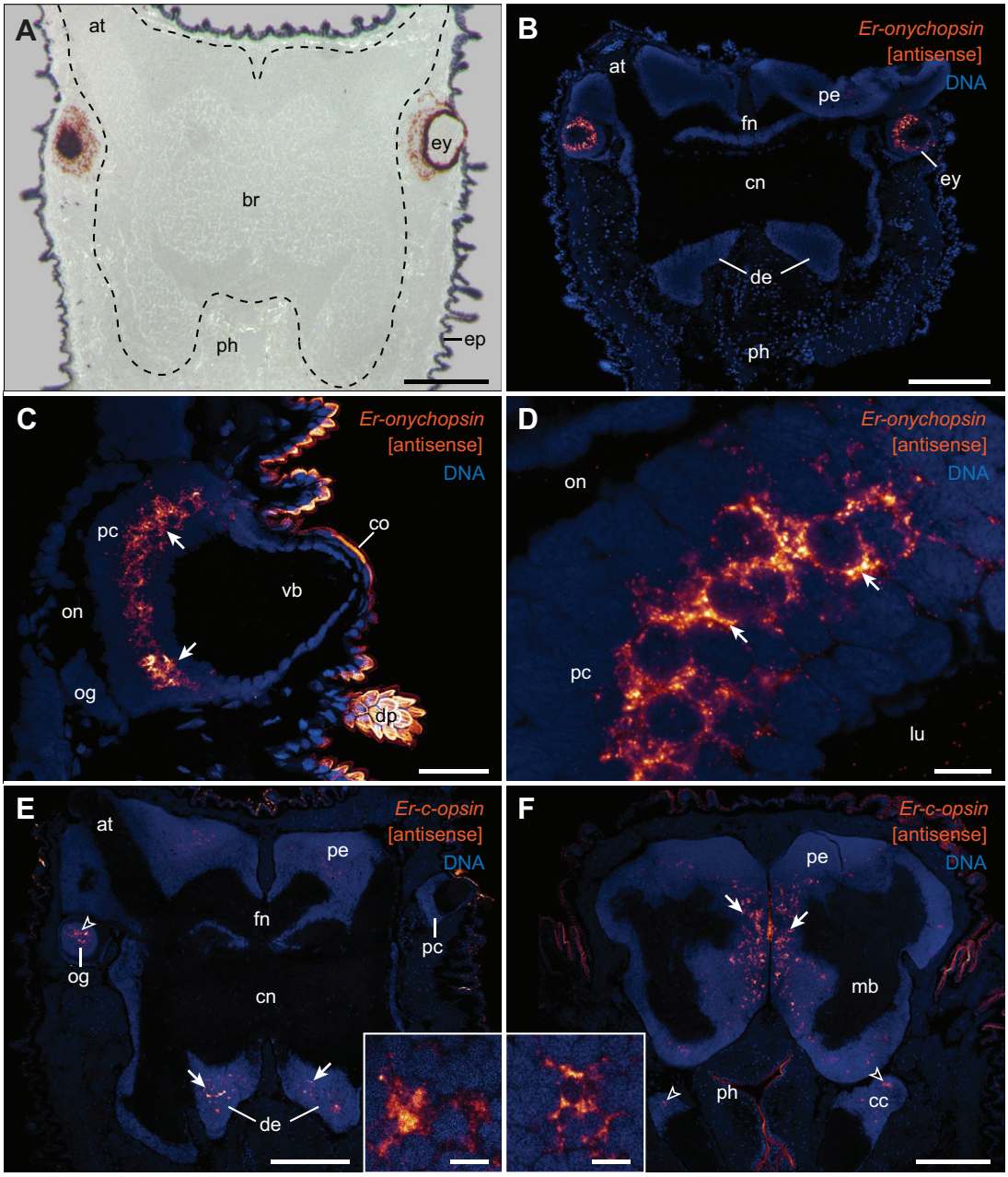

Fig. 4. Expression pattern of *Er-onychopsin* and *Er-c-opsin* mRNA in *E. rowelli* visualised using antisense probes. Horizontal sections of heads; anterior is up in all images. Light (A) and confocal micrographs (B–F) illustrating the results of fluorescence *in situ* hybridization experiments using antisense RNA probes which were visualised using fluorescein-labelled tyramide. DNA was stained using propidium iodide. (A) Cryosection showing the spatial relationship of the eyes to the brain (dashed line). (B) Section at the level of the eyes demonstrating the expression of *Er-onychopsin* in the eyes but not in the brain or other tissues. (C) Section of an eye showing that *Er-onychopsin* is expressed exclusively in the photoreceptor cell layer (arrows). The cuticle exhibits autofluorescence, which is also evident in sections labelled with the sense probe as a negative control (see supplementary material Fig. S2). (D) Detail of the photoreceptor cell layer. *Er-onychopsin* expression is restricted to the perikarya surrounding each nucleus (arrows). (E) Overview of *Er-c-opsin* expression in a section of the head at the level of the eyes. *Er-c-opsin* is expressed in the deutocerebrum (arrows) and in the optic ganglion cells (arrowhead) in the proximal portion of the eye (sectioned horizontally on the left side; see inset in the lower right corner for a higher magnification). Note the lack of signal in the photoreceptor cell layer of the eye on the right side. (F) Overview of *Er-c-opsin* expression in a section through the ventral part of the brain at the level of the mushroom bodies. *Er-c-opsin* is expressed in the median portion of the protocerebrum (arrows) and in the connecting cords linking the brain to the ventral nerve cord (arrowheads). Inset in the lower left corner shows detail of expression in the medioventral perikaryal layer within the protocerebrum. Abbreviations: at, antennal tract; br, brain; cn, central brain neuropil; cc, connecting cord; co, cornea; de, deutocerebrum; dp, dermal papilla; ep, epidermis; ey, eye; fn, frontal brain neuropil; lu, lumen of the eye vesicle; mb, mushroom body; og, optic ganglion cell layer; on, optic neuropil; pc, photoreceptor cell layer; pe, perikaryal layer of the brain; ph, pharynx; vb, vitreous body. Scale bars: 250 µm (A,B,E,F); 50 µm (C); 10 µm (D; insets in E,F).

rather than light, as there was no detectable increase of temperature in the arena even after illumination at maximum light intensity. The observed photonegative reaction is consistent with the nocturnal lifestyle and high susceptibility of onychophorans to desiccation (e.g. Manton and Ramsay, 1937; Bursell and Ewer, 1950; Eakin and Westfall, 1965; Read and Hughes, 1987). This might be one of the reasons why these animals generally avoid light, as it is a potential indicator of heat and low humidity.

The Journal of Experimental Biology (2015) 218, 915-922 doi:10.1242/jeb.116780

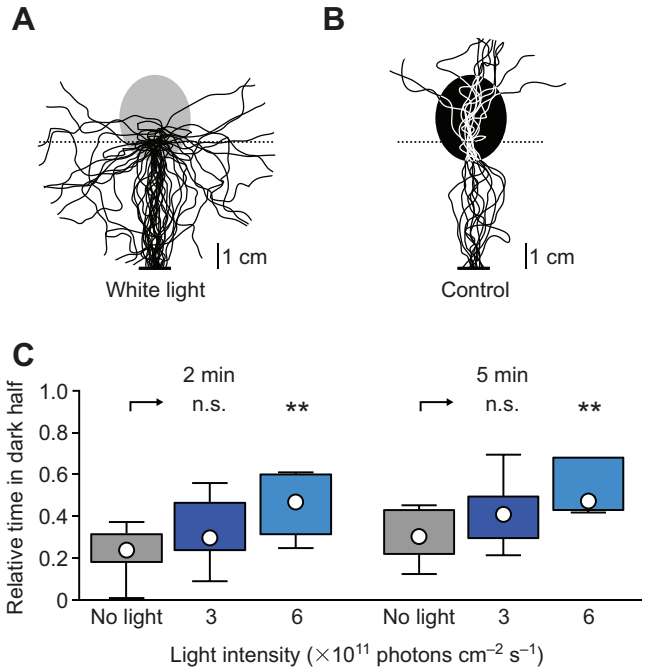

Fig. 5. Light-avoidance behaviour in the peripatopsid *E. rowelli*. (A) Bright white light was presented onto the head of each animal. Plotted paths of N=12 individuals of *E. rowelli* (Peripatopsidae), each tested twice (n=24). All animals change their walking direction and turn away from the light stimulus. (B) The paths of the same 12 animals are unaffected when no light was presented. The differences in turning are highly significant (P<0.001; Wilcoxon signed-rank test). (C) Sensitivity threshold of *E. rowelli* under 5 and 2 min of blue light illumination (λ_{max}=465 nm). Boxplots (N=7 groups of up to six animals, circles give the median, boxes the quartiles and whiskers represent 10/90 percentiles) illustrate the fraction of time spent in the dark half of the arena relative to the total time of the test. Significant avoidance reaction (**P<0.01; Friedman test with Dunn's post-test) occurs at an intensity of 6×10^{11} photons cm^{-2} s^{-1}, whereas no significant reaction is seen at 3×10^{11} cm^{-2} s^{-1} (n.s., not significant, P=0.570; Friedman test with Dunn's post-test).

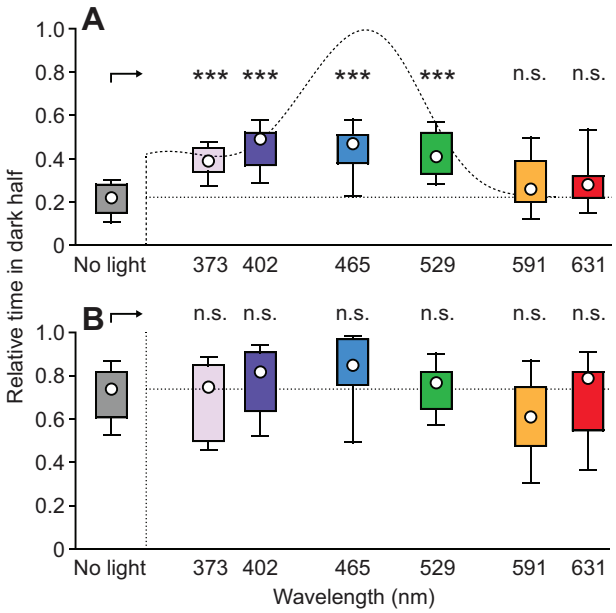

Fig. 6. Behavioural response to light stimuli of equal photon flux of different wavelengths in the peripatopsid *E. rowelli*. Groups (N=15) of up to six animals were stimulated for 2 min with a spectral light stimulus of 12×10^{11} photons cm^{-2} s^{-1}. In control experiments, the LEDs remained switched off. Friedman test with Dunn's post-test was used for data analysis. Boxplots (format as in Fig. 5) illustrating the fraction of time spent in the dark half of the arena relative to the total test time. Colours symbolise the wavelengths used. (A) Animals started in the illuminated half and showed negative phototactic behaviour to the light spectrum ranging from UV to green (***P<0.001), but not to longer wavelengths (P_{591}=0.343 and P_{631}=0.650; n.s., not significant). Every group is represented by a mean of three repetitions per wavelength. Dashed line indicates the average spectral sensitivity curve for *E. rowelli* obtained from electrophysiological recordings, with the baseline adjusted to the median of the behavioural control and the maximum standardised to 1. (B) Animals started in the dark half of the arena, while the other half was illuminated. No significant difference from the control is evident for any of the tested wavelengths (P_{465} and P_{591}=0.769, P_{others}>0.999). Dashed line indicates the median of the control.

The slow response of the onychophoran photoreceptors, as evidenced by a long time to peak and broad half width of the ERG signal in both species studied, is common in nocturnal invertebrates, which typically show slower reactions to light compared with diurnal animals. This is regarded as an adaptation to dim light conditions, because the long latency and response duration generally enhance the sensitivity of visual organs (reviewed by Warrant, 2008; Fain et al., 2010; Warrant and Dacke, 2011). According to our behavioural sensitivity tests, the threshold for negative phototaxis in *E. rowelli* lies at 6×10^{11} photons cm^{-2} s^{-1} for blue light. This value corresponds well to light intensities typically found on the ground of rainforests during the day (e.g. Vazquez-Yanes et al., 1990), which, again, is in line with the nocturnal lifestyle of velvet worms that usually forage for food at night and seek shelter during the day (Read and Hughes, 1987; Mesibov, 1998).

Previous behavioural data from the peripatid *P. hitoyensis* indicated that the maximum sensitivity in this species lies within the blue-green range of the light spectrum (Hering et al., 2012). Our results based on ERGs from the eyes of *P. hitoyensis* and *E. rowelli* now provide more precise values, and the estimated maxima at λ_{max}=474±6.5 nm in *E. rowelli* and λ_{max}=484 nm in *P. hitoyensis* suggest that the eyes of both species are most sensitive to blue light, i.e. close to the lower limit of the previously estimated range (cf. fig. 4 in Hering et al., 2012). A maximum sensitivity to blue light is widespread among invertebrates with monochromatic vision, which might be due to the maximum distribution of energy of solar radiation at about 480 nm (Menzel, 1979; Bowmaker and Hunt, 1999; Kelber and Roth, 2006).

Onychophorans exhibit monochromatic vision with onychopsin as the only visual opsin

The electrophysiologically determined spectral sensitivity of the dark-adapted eye could be well approximated assuming the presence of only one opsin-based visual pigment. Selectively adapting the retina to green light did not provide evidence for additional visual pigments maximally sensitive to shorter wavelengths. This finding is in line with the previous hypothesis of monochromatic vision in Onychophora, which is most likely based on an r-type opsin, the so-called onychopsin (Hering et al., 2012). However, since Eriksson et al. (2013) also detected a c-type opsin in the eye of *E. kanangrensis*, it was still debatable whether a c- or rather an r-type opsin is involved in onychophoran vision. Our *in situ* hybridization experiments in specimens of *E. rowelli* revealed *onychopsin* mRNA exclusively in the photoreceptor cell layer of the eye, but no expression in the brain (contrary to the claim of Eriksson et al., 2013) or other tissues. Conversely, we did not detect *Er-c-opsin* mRNA in the photoreceptor cells but rather in

The Journal of Experimental Biology (2015) 218, 915-922 doi:10.1242/jeb.116780

optic ganglion cells in the proximal portion of the eye as well as within the brain. In the brain, the majority of *Er-c-opsin*-positive somata occur in the ventromedian portion of the protocerebrum, but a few cell bodies are also found within the deutocerebrum. These findings, in particular the lack of *Er-c-opsin* expression in the photoreceptor cells, suggest that c-opsin is not involved in onychophoran vision. We therefore conclude that onychopsin is probably the only visual opsin in the onychophoran eye.

Although the function of the onychophoran c-opsin protein is unknown, it might be involved in non-visual, extraocular photoreception associated with circadian clock mechanisms (Fukada and Okano, 2002; Vigh et al., 2002; Arendt et al., 2004; Velarde et al., 2005; Shichida and Matsuyama, 2009). Notably, our expression data further indicate that the *Er-c-opsin* gene might be transcribed from both the sense and the antisense DNA strands, because our *in situ* hybridization experiments using the sense probe revealed a similar expression pattern of this gene to that using the antisense probe. The putative role of the *Er-c-opsin* antisense transcript in *E. rowelli* is unknown, but it might be involved in a self-regulation of *Er-c-opsin* expression – a function that has been suggested for other genes exhibiting antisense transcription (reviewed by Pelechano and Steinmetz, 2013).

Implications for the evolution of vision in Panarthropoda

Our electrophysiological data revealed maximum sensitivity to wavelengths around 480 nm in representatives of both major onychophoran subgroups, which suggests that the spectral absorption characteristics of the onychophoran photoreceptors in the retina have remained nearly unchanged for ∼350 million years, i.e. since the divergence of Peripatidae and Peripatopsidae (Murienne et al., 2014). This might be due to the generally conserved geographic distribution and lifestyle of onychophorans, which are confined to humid habitats and exhibit cryptic, nocturnal behaviour (Manton and Ramsay, 1937; Bursell and Ewer, 1950; Read and Hughes, 1987; Mesibov, 1998; Oliveira et al., 2012). In conclusion, our electrophysiological recordings, behavioural experiments and gene expression studies suggest that the onychophoran eye contains only one visual opsin, the r-type opsin onychopsin, which is most sensitive to blue light. C-opsin is restricted to the brain and may function in extra-ocular photoreception. Our data thus support the hypothesis of monochromatic vision in the last common ancestor of Panarthropoda (Hering et al., 2012; Hering and Mayer, 2014).

MATERIALS AND METHODS

Animals

Two species from the two major onychophoran subgroups were studied (Fig. 1A,B): *Principapillatus hitoyensis* Oliveira et al. 2012 (Peripatidae) and *Euperipatoides rowelli* Reid 1996 (Peripatopsidae). Specimens of *P. hitoyensis* were collected from leaf litter in the Reserva Biológica Hitoy Cerere (Province of Limón, Region of Talamanca, Costa Rica; 09°40′N, 83°02′W, 300 m). Specimens of *E. rowelli* were obtained from decaying logs in the Tallaganda State Forest (New South Wales, Australia; 35°26′S, 149°33′E, 954 m). Onychophorans were collected and exported under the following permits: (1) the Forestry Commission of New South Wales, Australia (permit no. SL100159); and (2) the Gerencia Manejo y Uso Sostenible de RR NN–Ministerio del Ambiente y Energia, Costa Rica (permit numbers 123-2005-SINAC and 014950). The animals were kept in plastic boxes with perforated lids, as described previously (Baer and Mayer, 2012). Specimens of *P. hitoyensis* were maintained at room temperature (20–24°C), whereas those of *E. rowelli* were kept at 18°C either in the dark (for behavioural experiments), in the dark and under day/night conditions (for gene expression studies), or under a shifted 14 h:10 h day:night cycle and tested in their active night period (in electrophysiological experiments). Behavioural experiments were carried out at a normal day/night rhythm between 4 and 9 pm at 19°C. Treatment of all animals complied with the Principles of Laboratory Animal Care and the German Law on the Protection of Animals.

Electroretinograms

To obtain ERGs, we fixed the anterior body portion of each specimen to a halved, tapered pipette tip (Fig. 2A) using dental silicone (polyvinyl siloxane, President light body, Iso 4823; Coltène, Altstätten, Switzerland) or a combination of dental silicone and a 1:1 mixture of beeswax and resin, taking care to leave one eye and its surroundings free. In most cases, it was necessary to immobilise the animal temporarily prior to handling with a 2–3 s pulse of carbon dioxide from a soda maker (Genesis, SodaStream, Tel Aviv, Israel). The reference electrode, a chlorinated silver wire, was brought in contact with the trunk of the specimen by conducting electrode paste (Gel101, Biopac Systems Inc., Goleta, CA, USA) and kept in place with paper tissue wrapped around the trunk and the pipette tip. To prevent dehydration, the tissue was soaked in saline based upon the composition of onychophoran haemolymph (Robson et al., 1966). Just posterior or dorsal to the exposed eye, the skin was thinned conically with the sharp tip of a broken razor blade. This allowed us to penetrate the integument with an electrolytically sharpened tungsten electrode for recording from the retina, while the skin closed tightly around the electrode and resealed the puncture (Fig. 2B).

A white light stimulus was produced by a 200 W Xenon lamp (Cermax LX175F ASB-XE-175EX, SP Spectral Products, Putnam, CT, USA) and directed to the eye via the central, 400-µm-wide fibre of a forked light guide (QR400-7-SR/BX, Ocean Optics, Dunedin, FL, USA), when two shutters (VS25S2ZM1R1 and LS6ZM2, both Uniblitz, Vincent Associates, Rochester, NY, USA) were opened. The angular position and distance of the tip of the light guide to the eye were adjusted on a goniometer such that the entire cornea was illuminated by the light beam of 16 deg divergence and ERG responses were maximised. Narrow-band interference filters (10–12 nm full width at half maximum; Melles Griot, Rochester, NY, USA) and neutral density filters (fused silica; also Melles Griot) could be inserted into the light path, providing spectral stimuli with equal photon flux from ultraviolet (330 nm) to red (700 nm) in 10 or 20 nm steps. All stimuli were delivered as flashes of 40 or 100 ms duration, separated by pauses of 3 or 5 s.

For spectral adaptation, light of a green light-emitting diode (LED) with a dominant wavelength of 521 nm and 34 nm full width at half maximum (LXHL-MM1D Green Luxeon Star, Quadica Developments Inc., Brantford, ON, Canada) was presented constantly throughout the experiment via the six outer fibres (each 400 µm in diameter) of the forked light guide. The combined light beam of 25 deg divergence provided between 3×10^{13} and 2×10^{16} photons cm^{-2} s^{-1} at the position of the eye, depending on the operating current of the LED and the distance between the cornea and the tip of the light guide.

Responses were amplified by a P15 AC amplifier (Natus Neurology Incorporated – Grass Technologies, Warwick, RI, USA) and sampled at 2000 Hz, digitised and saved using an NI PCIe-6251 data acquisition board and custom-made LabView scripts (both National Instruments Corporation, Austin, TX, USA) installed on a conventional computer.

All experiments were carried out in a darkened Faraday cage with either the stimulus or the stimulus and the spectral adaptation light as the only light source. Adaptation periods prior to recording had to be kept to a minimum (2–5 min for spectral adaptation and 5–10 min for dark adaptation) because of the reduced viability of the animals in the setup. The spectral sensitivity under dark adaptation was measured up to 10 times, alternating between series starting with short and proceeding to long wavelengths and series in the reverse order. Before and after each spectral series, a response–intensity (V–log I) relationship was determined to control for changes in recording quality and to establish the saturation level of responses. Initially, V–log I curves were measured with white light. When the peak sensitivity of an individual became evident, we used the available narrow-band spectral light closest to the presumed wavelength of maximal sensitivity for the V–log I. Up to three stable series in both directions, i.e. six series altogether, were selected per individual and analysed using custom-made scripts in Matlab (R2012b, The MathWorks, Natick, MA, USA) as described in detail elsewhere (Telles et al., 2014). In short, the ERG was smoothed by a moving average with a window width

The Journal of Experimental Biology (2015) 218, 915-922 doi:10.1242/jeb.116780

of 0.01 s. Response amplitudes were calculated as potential changes from the baseline at stimulus onset to maximal hyperpolarisation and converted into sensitivities based on the sigmoidal V–log I relationship obtained before and after each spectral series. We normalised all values to the maximal spectral sensitivity within a series and averaged series from the same individual. An established template for the absorbance of an opsin-based visual pigment (Govardovskii et al., 2000) was fitted to the entire mean spectral sensitivity curve using a non-linear least-squares approach. We varied the amplitude and wavelength of the α peak and the amplitude of the β peak independently. Since the sensitivity curve for wavelengths below 390 nm was too flat to determine the wavelength of the β peak, we calculated it as a function of the α peak, as suggested elsewhere (Govardovskii et al., 2000). Finally, the wavelengths of the estimated α peak (λ_{max}) and the respective coefficients of determination (R^2) were averaged for different individuals.

Fluorescence *in situ* hybridization

Partial sequences spanning most of the transmembrane region of the onychophoran r-type opsin [*Er-onychopsin*, 736 nt (CDS position 497–1232 of GenBank accession JN6613720)] as well as the c-type opsin [*Er-c-opsin*, 808 nt (KM189804)] were amplified from cDNA, which was obtained by reverse transcription of total RNA (Trizol extraction protocol) using Superscript II and DNA Pol I polymerase (Invitrogen, Carlsbad, CA, USA) according to the manufacturer's protocols. The fragments were cloned using the pGEM-T Vector System (Promega, Madison, WI, USA) and verified by Sanger sequencing (GATC Biotech, Konstanz, Germany). The cDNA clones were amplified by a standard M13 PCR and used directly to transcribe antisense and sense digoxigenin (DIG)-labelled RNA probes by using SP6 and T7 RNA polymerase, respectively, and the DIG RNA labelling mix (Roche Diagnostics, Rotkreuz, Switzerland). Freshly dissected heads of male specimens of *E. rowelli* (N=10) were embedded and immediately frozen in Tissue-Tek OCT Compound (Sakura Finetek, Europe B.V.) and 10- to 16-µm-thick horizontal sections were cut on a Cryostat CM3050 S (Leica Biosystems, Nussloch, Germany). The sections were mounted on SuperFrost plus slides (Menzel GmbH, Braunschweig, Germany), dried for 30 min at room temperature and fixed in 4% paraformaldehyde for another 30 min. After several washing steps with PBST (PBS with 0.1% Tween 20) and acetylation, the sections were pre-hybridised in hybridization buffer for 3–4 h at either 55°C or 58°C and then hybridised for 12–16 h at the same temperature using ∼1 ng µl^{-1} RNA probe. Hybridization was followed by multiple washing steps with saline-sodium citrate buffer (SSC with 0.1% Tween 20). The sections were incubated for 40 min in TNT buffer (0.1 mol l^{-1} Tris-HCl, pH 7.5; 0.15 mol l^{-1} NaCl; 0.1% Tween 20) containing 0.5% blocking reagent (PerkinElmer, Waltham, MA, USA). Anti-DIG-POD Fab-fragments (Roche Diagnostics), diluted either 1:50 or 1:100 in blocking solution, were then applied to the sections, which were incubated for additional 40–60 min at room temperature. After several washing steps with TNT buffer, the sections were incubated for 15 min with fluorescein-labelled tyramide (1:50 diluted working solution of the TSA Plus Fluorescein Fluorescence System; PerkinElmer). After counterstaining with propidium iodide for 15 min, the slides were mounted in Vectashield mounting medium (Vector Laboratories, Burlingame, CA, USA) and analysed with a confocal laser-scanning microscope (Leica TCS STED; Leica Microsystems). Confocal image stacks were processed with LAS AF Lite v2.4.1 (Leica Microsystems).

Behavioural experiments

The initial light-avoidance experiments to test for negative phototaxis were performed with single specimens of *E. rowelli* (N=12) as described previously for spectral experiments on *P. hitoyensis* (see Hering et al., 2012), except that only bright white light was presented. Each animal freely moved in a circular arena and its path was recorded 5 cm before and after stimulus presentation using the freely available video analysis and modelling tool Tracker (Douglas Brown, http://www.cabrillo.edu/~dbrown/; v.4.05). The paths of the animals tested were then plotted into a single diagram (Fig. 5A,B). The statistical analysis was conducted by comparing the turning angles of the animals under illumination to the control runs without the stimulus by applying the Wilcoxon signed-rank test (see Hering et al., 2012).

The remaining behavioural experiments were performed with a modified version of the setup introduced by Monge-Nájera et al. (1993) using a rectangular arena (163×93×70 mm) made of acrylic glass enclosed in black paper (Fig. 2C). A grey opaque, removable plastic plate separated the arena in two halves. One half could be illuminated by a cold light source via a double-ended light guide (Fig. 2C,D). For each experiment, the bottom of the arena was covered with a sheet of the same white paper towels that were used for maintaining the animals (Baer and Mayer, 2012). The sheet was folded three times, cut to the size of the arena and wetted with 5 ml distilled water, thus ensuring equal humidity in all experiments. No space was left between the paper towel and the border of the arena to prevent the animals from escaping under the paper towel.

All experiments were carried out in total darkness at 19.3±0.6°C. The light stimulus was delivered by narrow-banded LEDs (Nichia Corporation, Tokushima, Japan and Avago Technologies, San José, CA, USA). The LEDs emitted no light in the infrared range, and thus generated no detectable heat. To control for the possibility of the animals' reaction to heat rather than light, the temperature at the bottom of the arena was measured after illumination for 5 min with each LED at maximum intensity (i.e. for the 373, 402, 465, 528, 591 and 631 nm LEDs, the maximum intensity was 40, 220, 370, 130, 90 and 160 times higher than that used in our behavioural experiments, respectively). These measurements revealed no stimulus-correlated change in temperature. The stimulus was generated by the PowerLab 26T data acquisition system (AD Instruments, Dunedin, New Zealand) and equalised by using different output voltages and neutral density filters (Tinxi GmbH, Eggenstein–Leopoldshafen, Germany). Onset and offset of the stimulus was triggered with the Chart software (v5.5.6; AD Instruments). An infrared-sensitive camera (Sony Handycam HDR-HC7, Tokyo, Japan) was mounted above the arena to automatically record the experiments. To avoid potential bias caused by possible physical or chemical influence, such as smell, noise, heat or mechanical vibrations, all scoring and analyses were computerised and performed with the experimenter distant from the recording arena, except when releasing the animals. Before the next trial, the entire arena was cleaned and the paper towels renewed to remove any traces left by the animals. In addition, the entire setup was rotated by 90 deg every second day.

To determine the optimal duration and illumination intensity for the main behavioural experiments, seven groups of up to six specimens of *E. rowelli* (34 individuals in total) were dark-adapted for 20 min and placed in the illuminable half of the arena. After leaving them to settle for 2 min, the plastic plate separating the two halves was removed, the light switched on and each group tested for four different intensities (3×10^{11}, 6×10^{11}, 9×10^{11}, 12×10^{11} photons cm^{-2} s^{-1}) of the 465 nm blue light. The movements of the animals were recorded for 1, 2, 3 or 5 min (supplementary material Fig. S3).

These experiments revealed the optimal duration (2 min) and illumination intensity (twice the identified threshold, i.e. 12×10^{11} photons cm^{-2} s^{-1}), which were then used for the major behavioural experiments. For these experiments, narrow-band lights of six different wavelengths were used: 373±13 nm, 402 nm±10 nm, 465 nm±19 nm, 528 nm±26 nm, 591 nm±14 nm, and 631 nm±21 nm total width at half-maximum, respectively (Fig. 2E). As in the preliminary tests, up to six specimens were grouped (N=15 groups, 80 animals in total), dark-adapted for 20 min and tested in parallel. Each group experienced one run per day. In the tests for negative phototaxis (N=15 groups in total, three trials per wavelength), the animals were placed in the illuminable half of the arena, whereas in those for positive phototaxis (N=15 groups in total, one trial per wavelength) they were set in the dark half of the arena. The behaviour of the animals was recorded for 2 min after the light was switched on. Experiments in which animals interacted (e.g. pushed or bit each other, or aggregated) were not analysed and the animals were retested the following day (30 out of 410 experiments, 7.3%). To exclude potential biases, the wavelength of the presented light stimulus was changed randomly every day, only precluding the use of the neighbouring wavelengths in subsequent tests.

In all experiments, the time each animal spent in the dark half of the arena was measured, averaged for all specimens of the group and divided by the total experimental time. This resulted in a value ranging from 0 for no avoidance to 1 for total avoidance. The obtained data were analysed using

the non-parametric Friedman test, followed by Dunn's multiple comparison test to compare each wavelength against the control runs. These calculations were performed using the statistics program Prism v6 (GraphPad Software, La Jolla, CA, USA) and plotted with Adobe Illustrator CS5.1 (Adobe Systems, San José, CA, USA).

Acknowledgements
We are thankful to Noel Tait, David Rowell, Ivo de Sena Oliveira, Franziska Anni Franke, Michael Gerth and Sandra Treffkorn for help with specimen collection, to Ivo de Sena Oliveira for help with macrophotography, to Christine Martin for assistance with confocal microscopy, to Johanna Chavez and Martin Kohler for conducting behavioural pilot experiments, to Kerstin Flieger, Matthias Gilbert and Lars Thomas for help with calibrating the behavioural setup, to Klaus Schildberger, Dan-Eric Nilsson, Eric Warrant and Thomas Labhart for providing access to various equipment, to Ronald Petie for assistance in constructing the ERG setup, to David O'Carroll for valuable advice on the electrophysiological recording technique and to Uwe Mayer for helpful comments on the first draft of the manuscript. The staffs of the Forestry Commission of New South Wales (NSW, Australia), the Instituto Nacional de Biodiversidad (INBio, Costa Rica), and the National System of Conservation Areas (SINAC, MINAE, Costa Rica) are gratefully acknowledged for providing permits.

Competing interests
The authors declare no competing or financial interests.

Author contributions
H.B., P.A.S. and G.M. designed the behavioural experiments and H.B. carried out these experiments and analysed the data. M.J.H. and A.K. designed the electrophysiological experiments and H.B. and M.J.H. performed these experiments and analysed the data. L.H. and G.M. designed the gene expression experiments and L.H. carried out these experiments. G.M. and P.A.S. provided the setup and analysing tools for the behavioural experiments and A.K. contributed the electrophysiology setup. H.B. wrote the first draft and all authors read, made comments on and approved the final manuscript.

Funding
This work was supported by grants from the Studienstiftung des deutschen Volkes [German National Merit Foundation; 186861 to H.B.]; the Emmy Noether Programme of the German Research Foundation [Ma 4147/3-1 to G.M.]; and the K. & A. Wallenberg-Foundation and the Swedish Research Council [2012–2212 to A.K.].

Supplementary material
Supplementary material available online at
http://jeb.biologists.org/lookup/suppl/doi:10.1242/jeb.116780/-/DC1

References

Arendt, D., Tessmar-Raible, K., Snyman, H., Dorresteijn, A. W. and Wittbrodt, J. (2004). Ciliary photoreceptors with a vertebrate-type opsin in an invertebrate brain. *Science* **306**, 869-871.
Baer, A. and Mayer, G. (2012). Comparative anatomy of slime glands in Onychophora (velvet worms). *J. Morphol.* **273**, 1079-1088.
Bowmaker, J. K. and Hunt, D. M. (1999). Molecular biology of photoreceptor spectral sensitivity. In *Adaptive Mechanisms in the Ecology of Vision* (ed. S. N. Archer, M. B. A. Djamgoz, E. R. Loew, J. C. Partridge and S. Vallerga), pp. 439-462. Netherlands: Springer.
Briscoe, A. D. and Chittka, L. (2001). The evolution of color vision in insects. *Annu. Rev. Entomol.* **46**, 471-510.
Bursell, E. and Ewer, D. W. (1950). On the reactions to humidity of *Peripatopsis moseleyi* (Wood-Mason). *J. Exp. Biol.* **26**, 335-353.
Eakin, R. M. and Westfall, J. A. (1965). Fine structure of the eye of peripatus (Onychophora). *Z. Zellforsch. Mikrosk. Anat.* **68**, 278-300.
Eriksson, B. J., Fredman, D., Steiner, G. and Schmid, A. (2013). Characterisation and localisation of the opsin protein repertoire in the brain and retinas of a spider and an onychophoran. *BMC Evol. Biol.* **13**, 186.
Fain, G. L., Hardie, R. and Laughlin, S. B. (2010). Phototransduction and the evolution of photoreceptors. *Curr. Biol.* **20**, R114-R124.
Fukada, Y. and Okano, T. (2002). Circadian clock system in the pineal gland. *Mol. Neurobiol.* **25**, 19-30.
Giribet, G. and Edgecombe, G. D. (2012). Reevaluating the arthropod tree of life. *Annu. Rev. Entomol.* **57**, 167-186.
Govardovskii, V. I., Fyhrquist, N., Reuter, T., Kuzmin, D. G. and Donner, K. (2000). In search of the visual pigment template. *Vis. Neurosci.* **17**, 509-528.
Hering, L. and Mayer, G. (2014). Analysis of the opsin repertoire in the tardigrade *Hypsibius dujardini* provides insights into the evolution of opsin genes in Panarthropoda. *Genome Biol. Evol.* **6**, 2380-2391.
Hering, L., Henze, M. J., Kohler, M., Kelber, A., Bleidorn, C., Leschke, M., Nickel, B., Meyer, M., Kircher, M., Sunnucks, P. et al. (2012). Opsins in Onychophora (velvet worms) suggest a single origin and subsequent diversification of visual pigments in arthropods. *Mol. Biol. Evol.* **29**, 3451-3458.
Kelber, A. and Roth, L. S. V. (2006). Nocturnal colour vision – not as rare as we might think. *J. Exp. Biol.* **209**, 781-788.
Manton, S. M. and Ramsay, J. A. (1937). Studies on the Onychophora. III. The control of water loss in *Peripatopsis*. *J. Exp. Biol.* **14**, 470-472.
Mayer, G. (2006). Structure and development of onychophoran eyes: what is the ancestral visual organ in arthropods? *Arthropod. Struct. Dev.* **35**, 231-245.
Menzel, R. (1979). Spectral sensitivity and color vision in invertebrates. In *Comparative Physiology and Evolution of Vision in Invertebrates*, Vol. 7/6/6 A (ed. H. Autrum), pp. 503-580. Heidelberg; Berlin: Springer.
Mesibov, B. (1998). Curious, yes, but not all that rare. *Invertebrata* **11**, 6.
Monge-Nájera, J., Barrientos, Z. and Aguilar, F. (1993). Behavior of *Epiperipatus biolleyi* (Onychophora: Peripatidae) under laboratory conditions. *Rev. Biol. Trop.* **41**, 689-696.
Murienne, J., Daniels, S. R., Buckley, T. R., Mayer, G. and Giribet, G. (2014). A living fossil tale of Pangean biogeography. *Proc. R. Soc. B Biol. Sci.* **281**, 1471-2954.
Oliveira, I. S., Read, V. M. S. J. and Mayer, G. (2012). A world checklist of Onychophora (velvet worms), with notes on nomenclature and status of names. *ZooKeys* **211**, 1-70.
Pelechano, V. and Steinmetz, L. M. (2013). Gene regulation by antisense transcription. *Nat. Rev. Genet.* **14**, 880-893.
Porter, M. L., Blasic, J. R., Bok, M. J., Cameron, E. G., Pringle, T., Cronin, T. W. and Robinson, P. R. (2012). Shedding new light on opsin evolution. *Proc. R. Soc. B Biol. Sci.* **279**, 3-14.
Read, V. M. S. J. and Hughes, R. N. (1987). Feeding behaviour and prey choice in *Macroperipatus torquatus* (Onychophora). *Proc. R. Soc. B Biol. Sci.* **230**, 483-506.
Robson, E. A., Lockwood, A. P. M. and Ralph, R. (1966). Composition of the blood in Onychophora. *Nature* **209**, 533.
Shichida, Y. and Matsuyama, T. (2009). Evolution of opsins and phototransduction. *Philos. Trans. R. Soc. B Biol. Sci.* **364**, 2881-2895.
Stavenga, D. G. (2010). On visual pigment templates and the spectral shape of invertebrate rhodopsins and metarhodopsins. *J. Comp. Physiol. A* **196**, 869-878.
Telles, F. J., Lind, O., Henze, M. J., Rodríguez-Gironés, M. A., Goyret, J. and Kelber, A. (2014). Out of the blue: the spectral sensitivity of hummingbird hawkmoths. *J. Comp. Physiol. A* **200**, 537-546.
Vazquez-Yanes, C., Orozco-Segovia, A., Rincón, E., Sánchez-Coronado, M. E., Huante, P., Toledo, J. R. and Barradas, V. L. (1990). Light beneath the litter in a tropical forest: effect on seed germination. *Ecology* **71**, 1952-1958.
Velarde, R. A., Sauer, C. D., Walden, K. K. O., Fahrbach, S. E. and Robertson, H. M. (2005). Pteropsin: a vertebrate-like non-visual opsin expressed in the *honey bee* brain. *Insect Biochem. Mol. Biol.* **35**, 1367-1377.
Vigh, B., Manzano, M., Zádori, A., Frank, C., Lukáts, A., Röhlich, P., Szél, A. and Dávid, C. (2002). Nonvisual photoreceptors of the deep brain, pineal organs and retina. *Histol. Histopathol.* **17**, 555-590.
Warrant, E. (2008). Nocturnal vision. In *The Senses: A Comprehensive Reference* (ed. R. H. Masland, T. D. Albright, P. Dallos, D. Oertel, S. Firestein, G. K. Beauchamp, M. C. Bushnell, A. I. Basbaum, J. H. Kaas and E. P. Gardner), pp. 53-86. New York: Academic Press.
Warrant, E. and Dacke, M. (2011). Vision and visual navigation in nocturnal insects. *Annu. Rev. Entomol.* **56**, 239-254.

Supplementary material Fig. S1. Spectral adaptation of the eye of *Principapillatus hitoyensis*. ERG amplitudes in response to spectral flashes under dark adaptation (black, average +/- standard deviation, n = 4), adaptation to bright light of 521 nm (green, n = 1) and under recovery from spectral adaptation (grey, average +/- standard deviation, n = 4). The shape of the spectral curve under recovery is similar to the one of the dark-adapted eye except for overall lower amplitudes.

Supplementary material Fig. S2. Results of fluorescence *in situ* hybridization experiments for *Er-onychopsin* and *Er-c-opsin* in the peripatopsid *E. rowelli* using sense probes as a negative control. Confocal laser-scanning micrographs of horizontal cryosections of heads. DNA was stained using propidium iodide. Anterior is up and the cuticle is autofluorescent in both micrographs. (A) Detail of a horizontally sectioned eye. Note the lack of signal demonstrating that no *Er-onychopsin* antisense mRNA is localised in the eye. Scale bar: 50 µm. (B) In contrast, antisense transcription of *Er-c-opsin* is detectable in the ventral portion of the brain (arrows) as well as in the neuronal somata of the optic ganglion (arrowheads in the inset; inset scale bar: 50 µm). Scale bar: 250 µm. Abbreviations: cc, connecting cord (=medullary portion of the central nervous system linking the brain to the ventral nerve cord); co, cornea; dp, dermal papilla; mb, mushroom body; og, optic ganglion cell layer; on, optic neuropil; pc, photoreceptor cell layer; pe, perikaryal layer of the brain; ph, pharynx; vb, vitreous body.

Supplementary material Fig. S3. Determination of minimum stimulation time for behavioural experiments on the peripatopsid *E. rowelli*. Specimens (N=7 groups, 34 animals in total) were released in the illuminable half of the arena and their behaviour was recorded for 5 minutes under constant illumination with blue light (465 nm ± 19 nm total width at half-maximum) of different intensities. A significant light avoidance reaction was observed at 6×10^{11} photons cm^{-2} s^{-1} (Friedman-test with Dunn's post-test; significance levels: ** $p < 0.01$, ns no significance; circles give the median, boxes the quartiles, whiskers represent 10/90 percentiles). In order to reduce stress for the animals in subsequent experiments, their reaction to different illumination times was compared. A stimulation of 1 minute was already sufficient to induce a photonegative reaction without the loss of significance in the applied test statistics (see main text for further details).

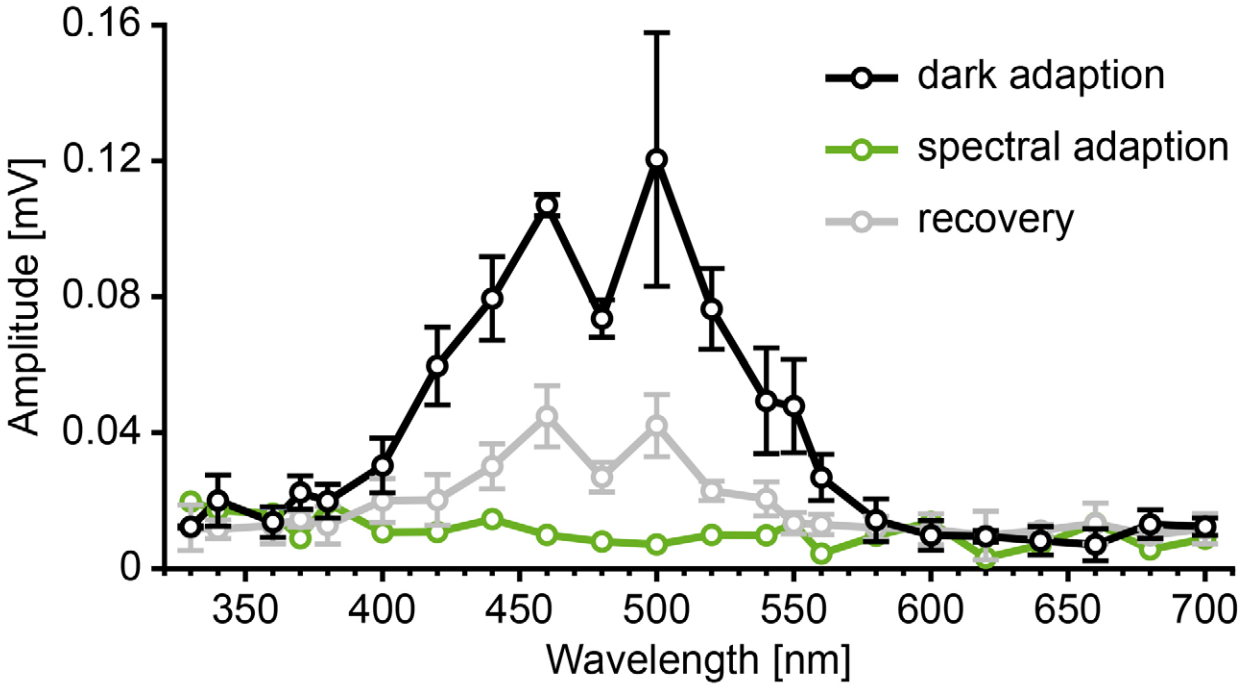

Figure S1

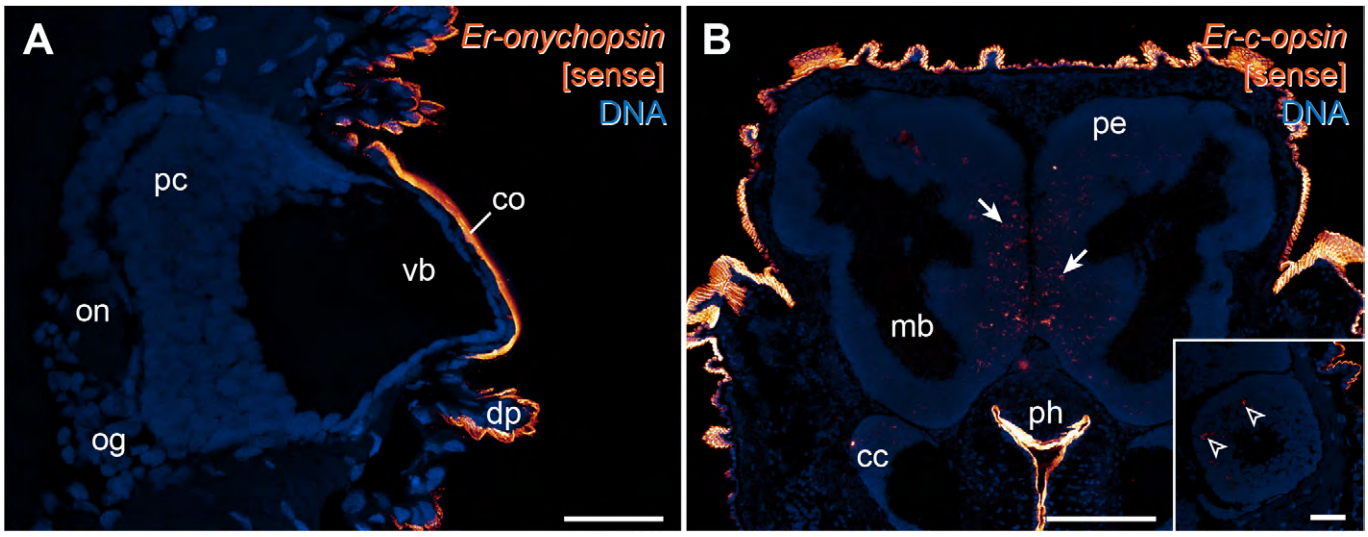

Figure S2

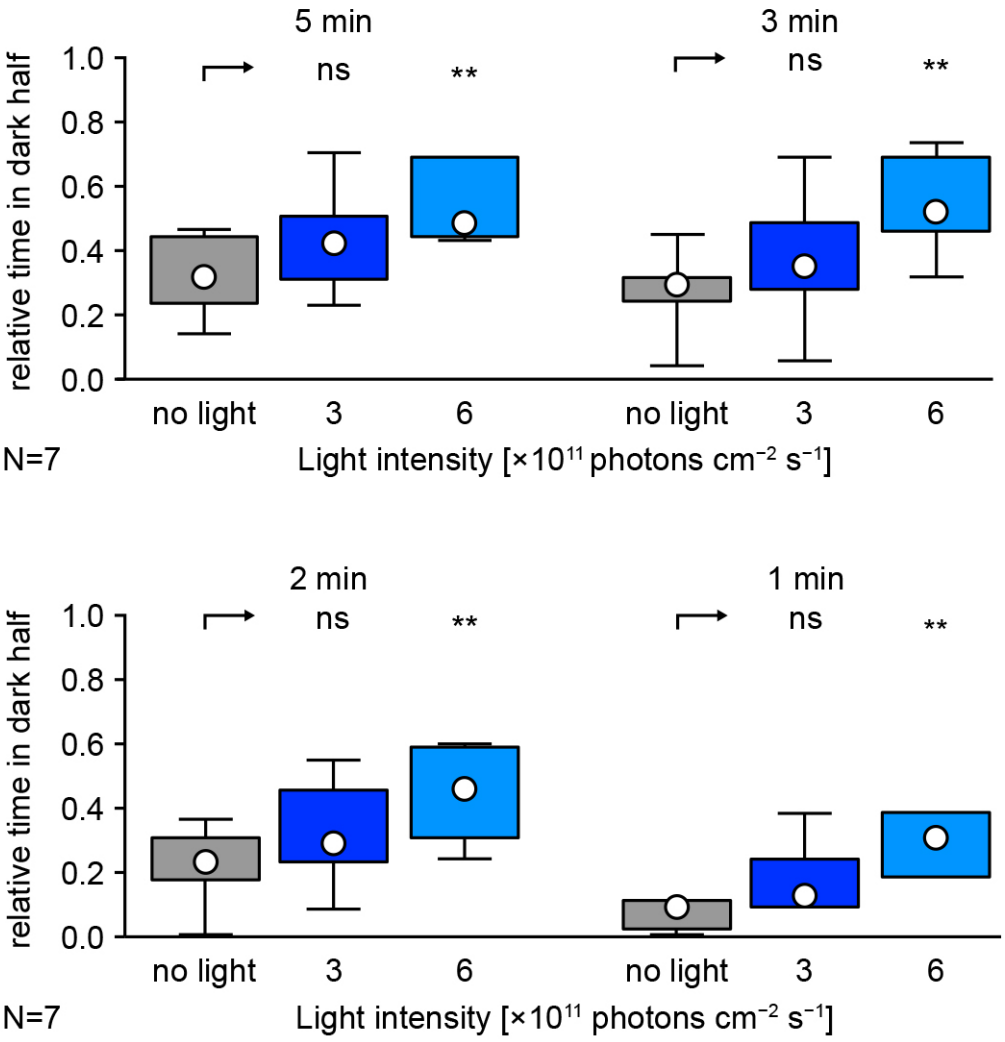
5 min
ns
**
3 min
ns
**
relative time in dark half
1.0
0.8
0.6
0.4
0.2
0.0
no light
3
6
no light
3
6
N=7
Light intensity [×10^11 photons cm^-2 s^-1]
2 min
ns
**
1 min
ns
**
relative time in dark half
1.0
0.8
0.6
0.4
0.2
0.0
no light
3
6
no light
3
6
N=7
Light intensity [×10^11 photons cm^-2 s^-1]

Figure S3